Liquid Crystals

ISSN: 0267-8292 (Print) 1366-5855 (Online) Journal homepage: https://www.tandfonline.com/loi/tlct20

Polarisation-dependent dielectric processes in ferroelectric liquid crystals

Ambika Bawa, Lokesh K. Gangwar, Aastha Dhingra, Amit Choudhary, Rajesh, Surinder P. Singh, Wolfgang Haase & Ashok M. Biradar

To cite this article: Ambika Bawa, Lokesh K. Gangwar, Aastha Dhingra, Amit Choudhary, Rajesh, Surinder P. Singh, Wolfgang Haase & Ashok M. Biradar (2019) Polarisation-dependent dielectric processes in ferroelectric liquid crystals, Liquid Crystals, 46:2, 166-175, DOI: 10.1080/02678292.2018.1480805

To link to this article: https://doi.org/10.1080/02678292.2018.1480805

Published online: 11 Jun 2018.

LIQUID CRYSTALS
2019, VOL. 46, NO. 2, 166–175
https://doi.org/10.1080/02678292.2018.1480805

Taylor & Francis
Taylor & Francis Group

Polarisation-dependent dielectric processes in ferroelectric liquid crystals

Ambika Bawa[a,b], Lokesh K. Gangwar[a,b], Aastha Dhingra[b], Amit Choudhary[c], Rajesh [b], Surinder P. Singh[b], Wolfgang Haase[d] and Ashok M. Biradar[b]

[a]Academy of Scientific and Innovative Research (AcSIR), CSIR- National Physical Laboratory (CSIR-NPL) campus, New Delhi, India; [b]CSIR-National Physical Laboratory, Dr. K. S. Krishnan Marg, New Delhi India; [c]Physics Department, Deshbandhu College (University of Delhi), New Delhi, India; [d]Department of Physical Chemistry, Darmstadt University of Technology, Darmstadt, Germany

ABSTRACT

The behaviour of dielectric relaxation process has been investigated in four ferroelectric liquid crystal (FLC) materials having different spontaneous polarisation (*Ps*) values. *Ps* effect on the permittivity in four different FLCs has been carried out in highly anchored sample cells around ~8 µm thick. It has been found that the main contribution to the dielectric permittivity in chiral Smectic C (SmC*) phase is due to Goldstone mode (GM) and partially unwound helical mode (*p*-UHM). In higher *PS* value FLC materials, the *p*-UHM process is found to dominate the dielectric properties. It has also been observed that *p*-UHM process is highly dependent on the probing ac voltage and temperature, whereas GM is found to be weakly dependent of probing voltage and temperature in SmC* phase of all the studied FLC materials. The influential contribution of *p*-UHM has exhibited the dielectric properties in its intrinsic frequency range making the materials suitable for futuristic display and photonics devices.

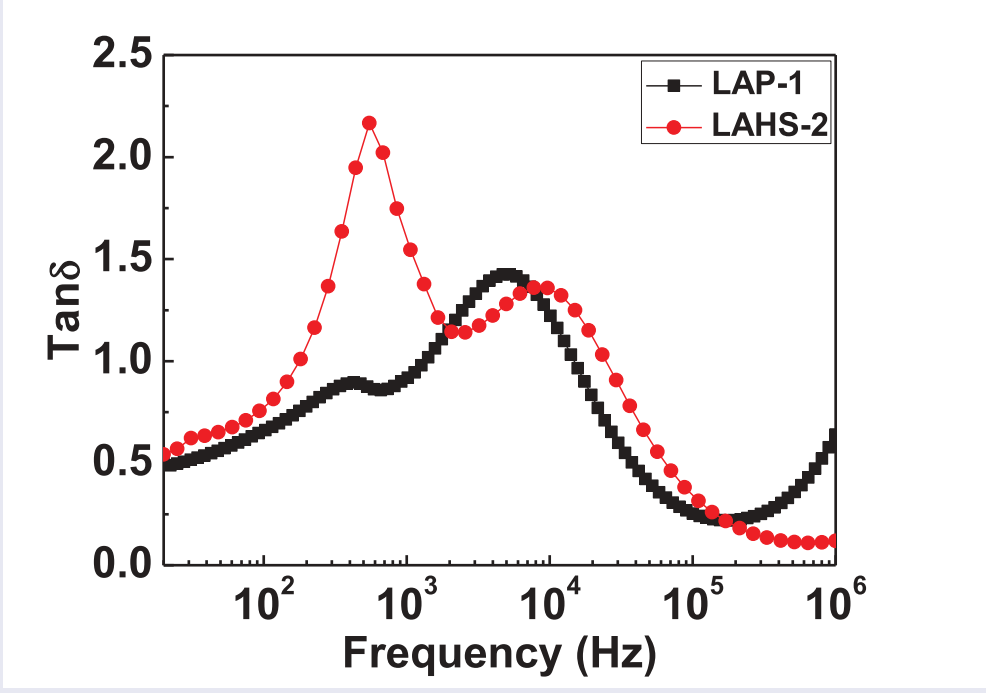

ARTICLE HISTORY
Received 14 March 2018
Accepted 21 May 2018

KEYWORDS
Ferroelectric liquid crystal; dielectric; spontaneous polarization; phase transition

Introduction

Chiral Smectic C (SmC*) ferroelectric liquid crystal (FLC) materials are one of the most promising phases of liquid crystalline family. However, the devices based on FLCs are scarcely available in the market because of the fact that there are some basic problems which are not well understood yet, like alignment of these molecules and molecular dynamics in thick and thin cells [1–4]. The understanding of the molecular dynamics in various configurations (thick and thin cells) leads the materials for practical applications. The dielectric

CONTACT Amit Choudhary abiradar.npl@gmail.com; amitnpl2005@gmail.com

spectroscopy of FLCs plays a crucial role in deciding the applicability of the FLC material for practical application like the alignment (vertical or planar) can be decided by performing dielectric spectroscopy and knowing the type of dielectric anisotropy (positive or negative) and hence influences applied aspects of display devices. The understanding of collective/molecular relaxation phenomenon is significant in knowing the dynamical functionality of FLC molecules in the technological implementation of FLCs.

The FLC materials for understanding molecular dynamics are mainly characterised by elctro-optical and dielectric spectroscopy that reveals mainly two dielectric modes in SmC* phase, called Goldstone mode (GM) and soft mode processes. These two modes appear due to phase fluctuations and tilt angle fluctuations of FLC molecules, respectively. The soft mode in SmC* phase appears in very narrow temperature range near the transition temperature of SmC* to SmA phase as the tilt angle fluctuations are maximum. Phason mode (i.e. GM) appears throughout the SmC* phase having higher dielectric permittivity as compared to the other processes in this phase. A rich literature on dielectric processes of FLCs is available where the behaviour of GM with temperature has been studied in SmC* phase [5–7]. The ambiguity still persists in the literature whether the behaviour of dielectric strength ($\Delta\varepsilon$) of GM process is in the trend of increasing or continuously decreasing in SmC* phase and in the vicinity of SmC* to SmA phase transition. This might be because of the fact that the helical structure in the sample geometry is not taken into account [8–10].

From application point of view, the surface-stabilised structure FLC has shown potential towards memory application of FLC materials due to the suppression of helical structure [11,12]. Dielectric spectroscopy of FLC material in the confined geometry of the aero gels has shown that its $\Delta\varepsilon$ is about 1/3 times of maximum $\Delta\varepsilon$ of bulk FLC system [13]. The helical structure within the pores of aero gel is distorted and is supposed to reduce the $\Delta\varepsilon$ of the FLC system. The dielectric relaxation process due to collective director fluctuations close to phase transition of FLC is observed under the constraint of suppression of helix. The dielectric increment has been found decreasing in SmC* phase when cell thickness is increased whereas it is found increasing in SmA phase. The results are attributed as the consequences of the splayed structure of the FLC layers [14]. These observations clearly indicate that helical structure is also a very significant part for understanding the properties of FLCs.

The geometry of the FLC system could play an important role in varying the dielectric properties such as $\Delta\varepsilon$ and dielectric relaxation processes. Recently, it has been observed that helical structure also plays an important role in contributing to the dielectric permittivity in SmC* phase [15,16]. This is due to partially unwound helical structure called partially unwound helical mode (*p*-UHM); of course, this mode is strongly correlated with phase fluctuation mode.

In present article, we report dielectric behaviour of our FLC materials [two FLCs and two deformed helix FLCs (DHFLCs)] in strongly anchored sample cells systems in which the surface helical structure is partially unwound whereas the bulk helix is supposed to form complete helical structure. The FLC materials differ in the spontaneous polarisation (*Ps*) in SmC* phase. The materials are chosen that the other parameters like thickness of the cell, surface anchoring, applied electric field and ambient temperature are kept uniform for all the studied materials. Four FLC materials were selected of which two are conventional FLCs and other two are short pitch DHFLC materials. It has been observed in the present study that the main contribution to the dielectric permittivity in SmC* phase is due to GM and partially unwound helix modes [15]. In low *Ps* value FLC materials, the GM contribution is more than *p*-UHM process, and in higher *Ps* value FLC materials, *p*-UHM process dominates GM process.

Experimental

Four FLC materials having following *Ps*, pitch values (*h*), and viscosity (η;) and phase sequences are given in the Table1.

Phase Sequences of materials as determined by differential scanning calorimetry (DSC):

Table 1. Various parameters of FLCs and DHFLCs at room temperature (25°C).

Material	*Ps* (nC/cm^2)	Pitch (μm)	2θ tilt (25°C)	Viscosity at 25°C (mPa.S)
Felix 17/000 (FLC)	~9.5	~2	51.6°	47
Felix 17/100 (FLC)	~47	~3	55.1°	116
LAP-1[a] (DHFLC)	~26	0.8	38°	1000
LAHS-2[a] (DHFLC)	~47	0.8	46°	2000

[a]Synthesised by Prof. Haase's Group at Darmstadt, Germany.

$$\text{Felix } 17/000 : \text{Cryst.} \overset{-26^{\circ}\text{C}}{\leftrightarrow} \text{SmC}^{*} \overset{70^{\circ}\text{C}}{\leftrightarrow} \text{SmA} \overset{76^{\circ}\text{C}}{\leftrightarrow} \text{N} \overset{84-87^{\circ}\text{C}}{\leftrightarrow} \text{Iso.}$$

$$\text{Felix } 17/100 : \text{Cryst.} \overset{-28^{\circ}\text{C}}{\leftrightarrow} \text{SmC}^{*} \overset{73^{\circ}\text{C}}{\leftrightarrow} \text{SmA} \overset{77^{\circ}\text{C}}{\leftrightarrow} \text{N} \overset{84-87^{\circ}\text{C}}{\leftrightarrow} \text{Iso.}$$

$$\text{LAP} - 1 : \text{Cryst.} \overset{?}{\leftrightarrow} \text{SmC}^{*} \overset{56.5^{\circ}\text{C}}{\leftrightarrow} \text{SmA} \overset{66.4^{\circ}\text{C}}{\leftrightarrow} \text{Iso.}$$

$$\text{LAHS} - 2 : \text{Cryst.} \overset{?}{\leftrightarrow} \text{SmC}^{*} \overset{58^{\circ}\text{C}}{\leftrightarrow} \text{SmA} \overset{62.5^{\circ}\text{C}}{\leftrightarrow} \text{Iso.}$$

Here question mark '?' represents the unavailability of crystalline to SmC* phase transition temperature [17].

Highly conducting ITO-coated glass plates (~20 Ω/□) were used for making the sample cells. The effective electrode area of 0.4 × 0.4 cm^2 was etched by photographic technique. Nylon (6/6) was coated on the electrode and strongly rubbed along the desired direction for planar-aligned cells. The two electrodes were assembled using a Mylar spacer of thickness ~8 μm. The FLC material was introduced in the cell by means of capillary action by heating the material at its isotropic phase and cooled slowly to room temperature. The alignment of the liquid crystal molecules was confirmed under crossed polarising microscope (Carl Zeiss, Axioskop 40A, Oberkochen, Germany) for its planar alignment. The dielectric measurements were performed using an impedance analyzer instrument (Wyne Kerr, precision impedance analyzer, 6540A, West Sussex, UK) in the frequency range of 20 Hz–1MHz. The temperature controller (JULABO, 25 HE, Seelbach, Germany) was used for different temperature studies, having the temperature accuracy of ±0.1°C. The phase sequence of newly synthesised LAP-1 material is confirmed by DSC [Figure 1].

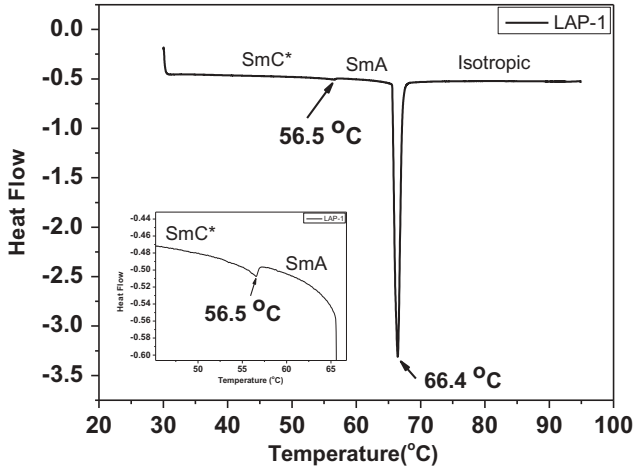

Figure 1. Differential scanning calorimetry (DSC) of LAP-1 DHFLC.

Result and discussion

Dielectric behaviour at room temperature

The dielectric spectroscopy of *p*-UHM process is presented in two conventional FLCs and two DHFLCs having different *Ps* values, whereas other parameters like thickness of the cell, surface anchoring, applied electric field and ambient temperature are maintained uniform for all materials. The dielectric permittivity (ε′) and loss factor (tanδ) of FLCs (Felix-17/000 and Felix-17/100) and two short pitch DHFLCs (LAP-1 and LAHS-2 [17]) as a function of frequency in all four materials at 100 mV probing ac voltage at temperature have been presented in Figure 2. As seen in Figure 2(a), the permittivity at low frequency is around four times more in Felix 17/100 FLC having high value of *Ps* as compared to low *Ps* value material (Felix 17/000). Even the relaxation frequency in tanδ and ε″ for high-value *Ps* FLC is observed at higher frequency value as shown in Figure 2(b,c). Similar is the case for DHFLC materials having different *Ps* values as shown in Figure 2(d–f). If one sees carefully tanδ versus frequency curves, Figure 2(b,e), in all the four materials, a single peak is observed at 100 mV probing ac voltage which is due to the phase fluctuation mode called GM. The only difference for high-value *Ps* materials is the relaxation frequency of GM appears at higher frequency [Figure 2(e)]. The same observation is in the result of ε″ versus frequency, Figure 2(f). However, the relaxation frequency peak in ε″ is found shifted to lower frequency value as per the rule $\nu = \nu_{\tan\delta}\sqrt{\frac{\varepsilon_{\infty}}{\varepsilon_0}}$, where $\nu_{\tan\delta}$ is the relaxation frequency observed from the tanδ versus frequency curves and ν is the relaxation frequency observed from the ε″ versus frequency curves. ε_{∞} and ε_0 are the real part of complex dielectric permittivity at high and low frequencies. As seen in figure, the relaxation frequency in FLCs appear in few hundred hertz, and in DHFLC materials, it appears in kHz range because of the fact that DHFLC materials have very high *Ps*, viscosity and very short pitch value.

The dielectric spectroscopy of FLCs and DHFLCs at 500 mV probing ac voltage at room temperature has shown an increment in the dielectric permittivity. An additional relaxation process in DHFLCs as discussed above, called *p*-UHM process, is observed at a lower frequency than GM, Figure 3. In FLCs [Figure 3(a)], the higher *Ps* value material Felix-17/100 FLC has attained higher relative dielectric permittivity value (ε′) of GM than Felix-17/000. The GM relaxation peak of Felix-17/100 in tanδ graph and ε″ are also at higher

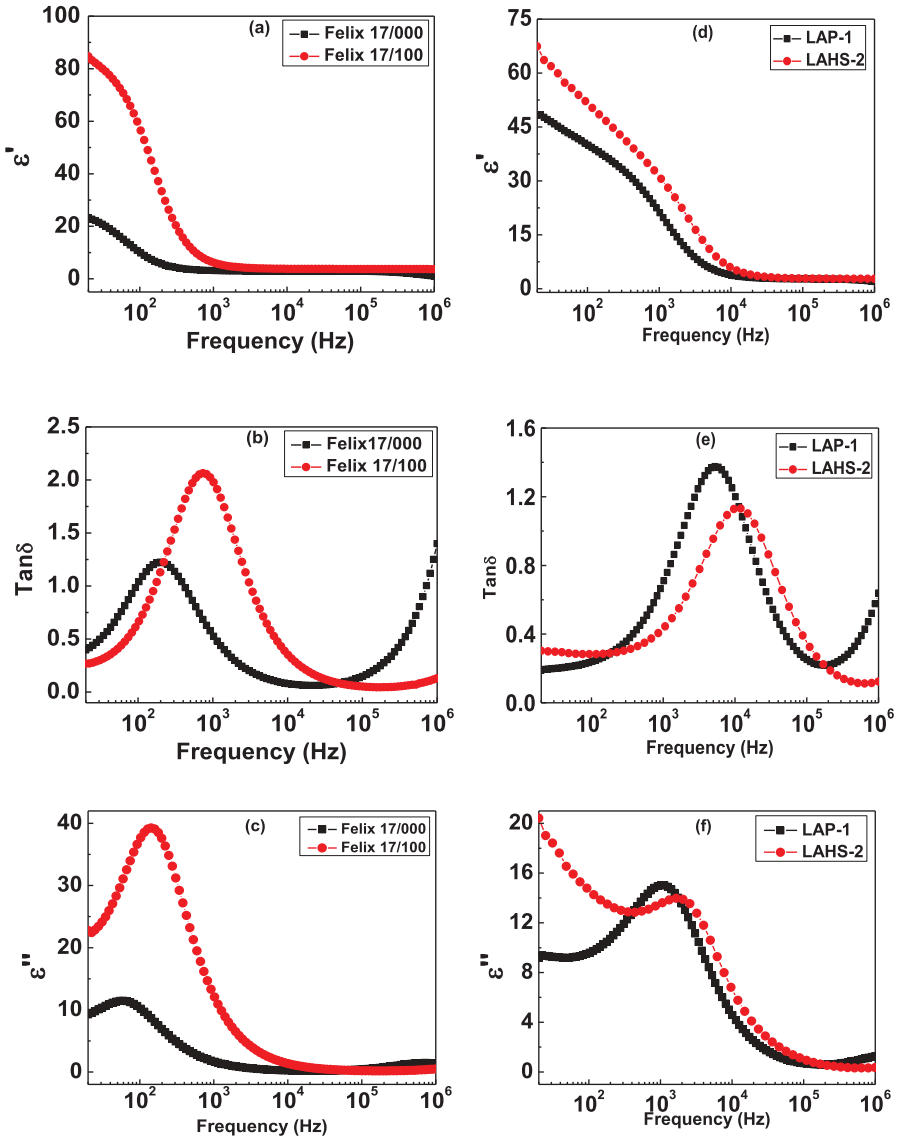

Figure 2. (Colour online) Dielectric spectroscopy at 100 mV probing ac voltage. (a) real part of dielectric permittivity of FLCs (Felix-17/000 and Felix17/100), (b) tanδ as a function of frequency of FLCs (Felix-17/000 and Felix-17/100), (c) Imaginary part of complex dielectric permittivity of FLCs (Felix-17/000 and Felix-17/100), (d) real part of dielectric permittivity of DHFLCs (LAHS-2 and LAP-1) and (d) tanδ as a function of frequency of DHFLCs (LAHS-2 and LAP-1) and (e) imaginary part of complex dielectric permittivity of DHFLCs (LAHS-2 and LAP-1).

frequency than Felix-17/000 as shown in Figure 3(b,c). On the other hand in DHFLCs [Figure 3(d)], the LAHS-2 having higher *Ps* value has attained a higher value of permittivity at lower frequency range than lower *Ps* value LAP-1.The increase in permittivity in both the DHFLCs is more than twice at 500 mV probing ac voltage which means at higher probing field, there could be some other dielectric process responsible for the increase in permittivity other than the GM process. Indeed, the *p*-UHM is clearly seen in the tanδ and ε″ versus frequency curves [Figure 3(e,f)] in both the DHFLCs [16]. The GM relaxation frequency is in kHz range but the *p*-UHM peak is in few hundred Hertz frequency range. In high *Ps* value LAHS-2, the magnitude of *p*-UHM process is more than GM which is responsible for the huge increase in the permittivity at 500 mV probing ac voltage. In low *Ps* value LAP-1, the *p*-UHM process is clearly observed but not as dominant as in high *Ps* material as seen in Figure 3(d). The *p*-UHM process could not be detected in FLC material at higher probing field at room temperature as seen in Figure 3(b). However, at higher temperatures this process has been detected clearly in Felix 17/100 which will be discussed in the further sections. In the observation so far, it has been found that the effect of surface anchoring is more conspicuous in high *Ps* materials.

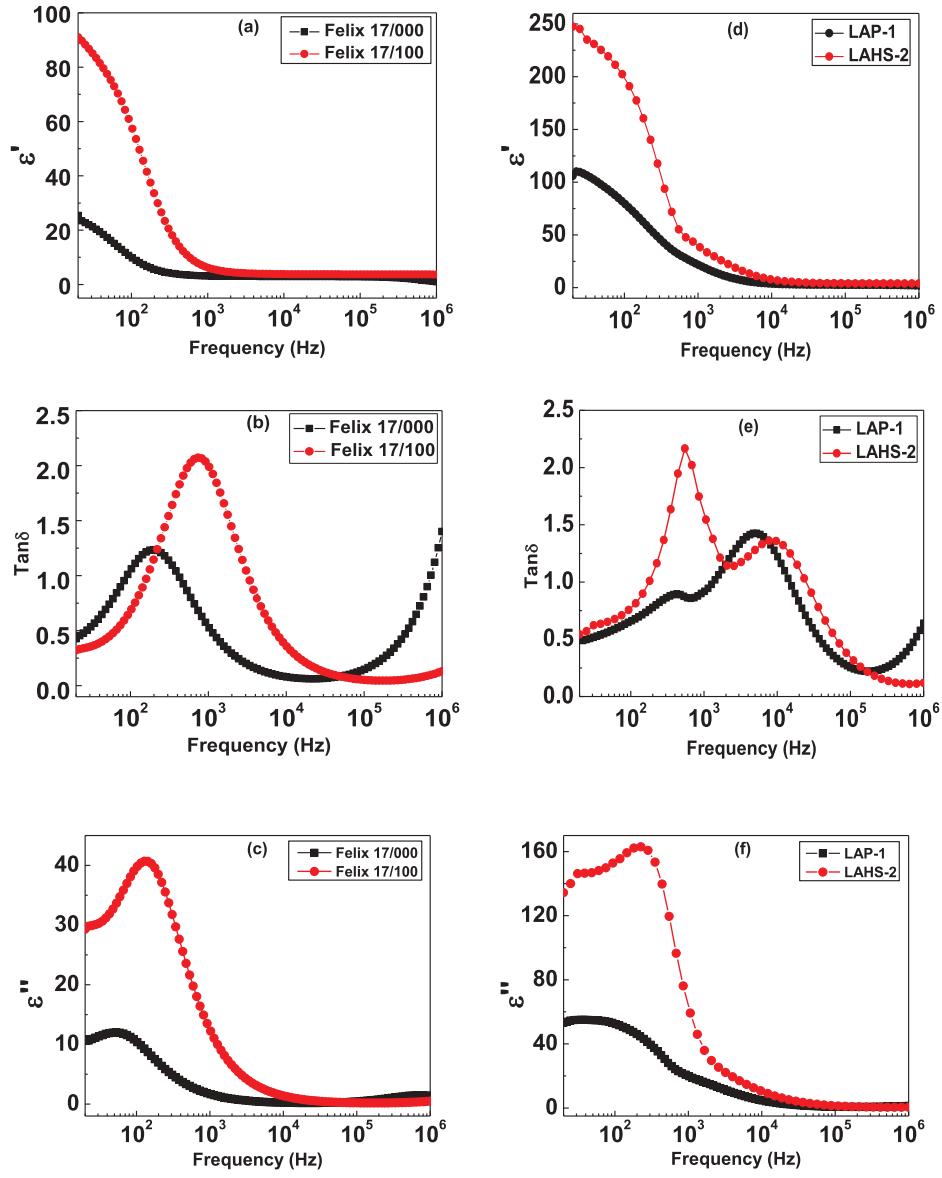

Figure 3. (Colour online) Dielectric spectroscopy at 500 mV probing ac voltage. (a) real part of dielectric permittivity of FLCs (Felix-17/000 and Felix17/100), (b) tanδ as a function of frequency of FLCs (Felix-17/000 and Felix-17/100), (c) Imaginary part of complex dielectric permittivity of FLCs (Felix-17/000 and Felix-17/100), (d) real part of dielectric permittivity of DHFLCs (LAHS-2 and LAP-1) and (d) tanδ as a function of frequency of DHFLCs (LAHS-2 and LAP-1) and (e) imaginary part of complex dielectric permittivity of DHFLCs (LAHS-2 and LAP-1).

Temperature-dependent behaviour

The Δε of GM and *p*-UHM process is studied at two different probing ac voltages for various temperatures in SmC* phase of FLC and DHFLC materials. As seen in Figure 4, the Δε is low at lower temperature (~35°C) and almost constant with temperature for low *Ps* value Felix 17/000 at 100 mV field, whereas for the other Felix 17/100, the trend is almost the same but the only difference in high *Ps* value, that is, the Δε is very large as compared with low *Ps* material [Figure 4(a)]. In DHFLC material, Figure 4(b), the behaviour of Δε is not as in FLCs at low temperature (~35°C) but it is observed increasing with temperature and decreases near transition temperature (T_c) shown in Figure 4 (b). This means that there might be active *p*-UHM process other than the GM in high *Ps* value DHFLC materials resulting into the high Δε just below the T_c of SmC* to SmA phase transition. A reduction has also been seen in transition temperature as compared to DSC transition temperature of all materials due to strong surface anchoring effect, also observed by Takezoe et al. and Pikin et al. [18,19]

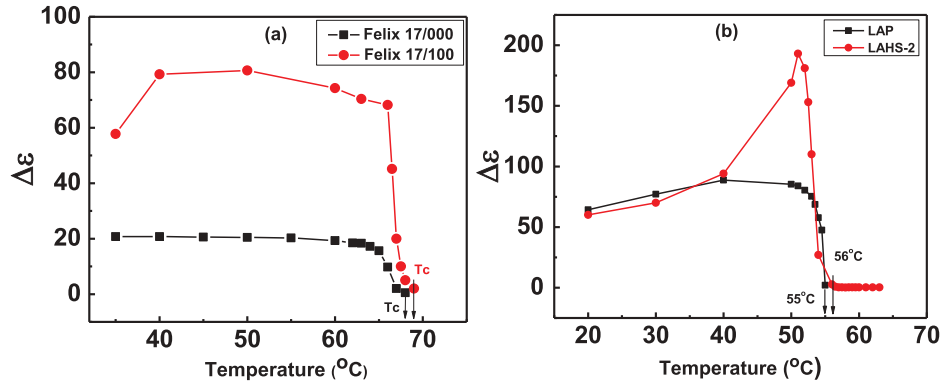

Figure 4. (Colour online) Dielectric strength of (a) FLCs and (b) DHFLCs as function of temperature at 100 mV probing ac voltage.

Figure 5(a) shows the Δε in FLCs at 500 mV probing ac voltage for various temperatures. The behaviour of Δε at 500 mV in low *Ps* material (Felix-17/000) is almost the same as that of 100 mV data [Figure 4(a)]. In higher *Ps* FLC material, the Δε at 500 mV is more than Δε at 100 mV for the same material. But it is higher than the lower *Ps* FLC, which is due to the contribution from *p*-UHM process and seen clearly in the tanδ versus frequency at higher temperatures (60°C and 65°C). The relaxation process at higher frequency is due GM, and at lower frequency, it is *p*-UHM as shown in Figure 5(b). The same processes are observed in the ε″ versus frequency curves but at lower frequencies as discussed above, Figure 5(c).

In DHFLCs, the Δε at 500 mV probing ac voltage, at different temperatures, the variation in the properties is larger as compared to FLCs Figure 6(a). It is interesting to see in both DHFLCs that at 500 mV applied voltage. The Δε of DHFLC (LAP-1) is maximum at room temperature (35° C) and then starts decreasing with temperature. This means that when both the modes (GM and *p*-UHM) are clearly separated, the dielectric permittivity at lower

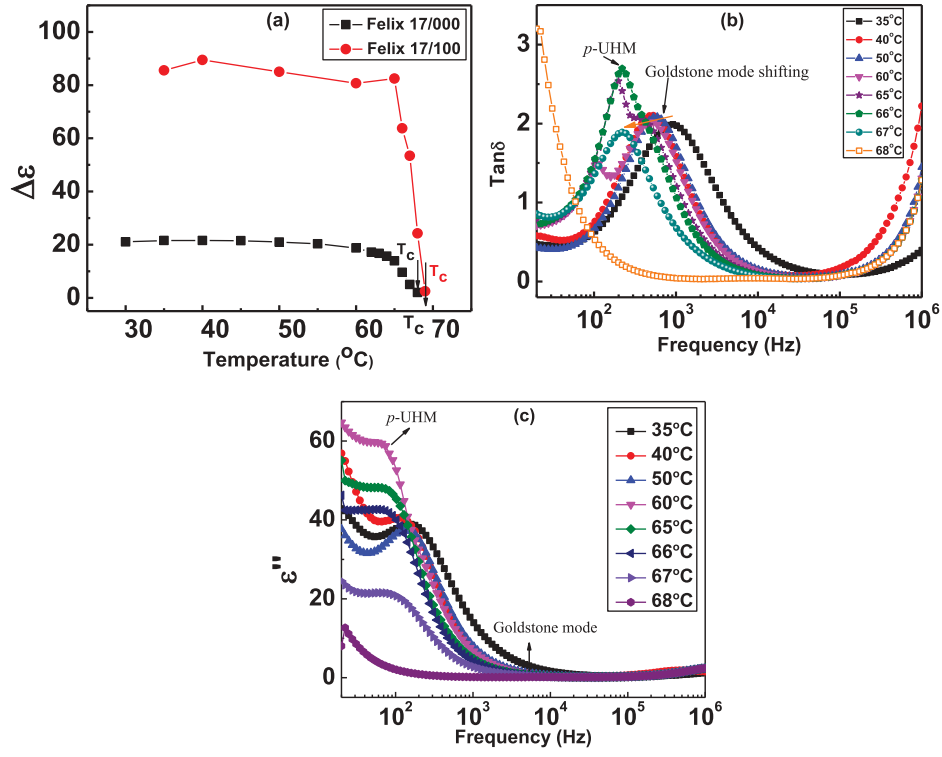

Figure 5. (Colour online) (a) Dielectric strength of FLCs at 500 mV, (b) tanδ at 500 mV as a function of frequency in Felix 17/100 at different temperatures and (c) the imaginary part of complex dielectric permittivity at 500 mV as function of frequency at different temperatures.

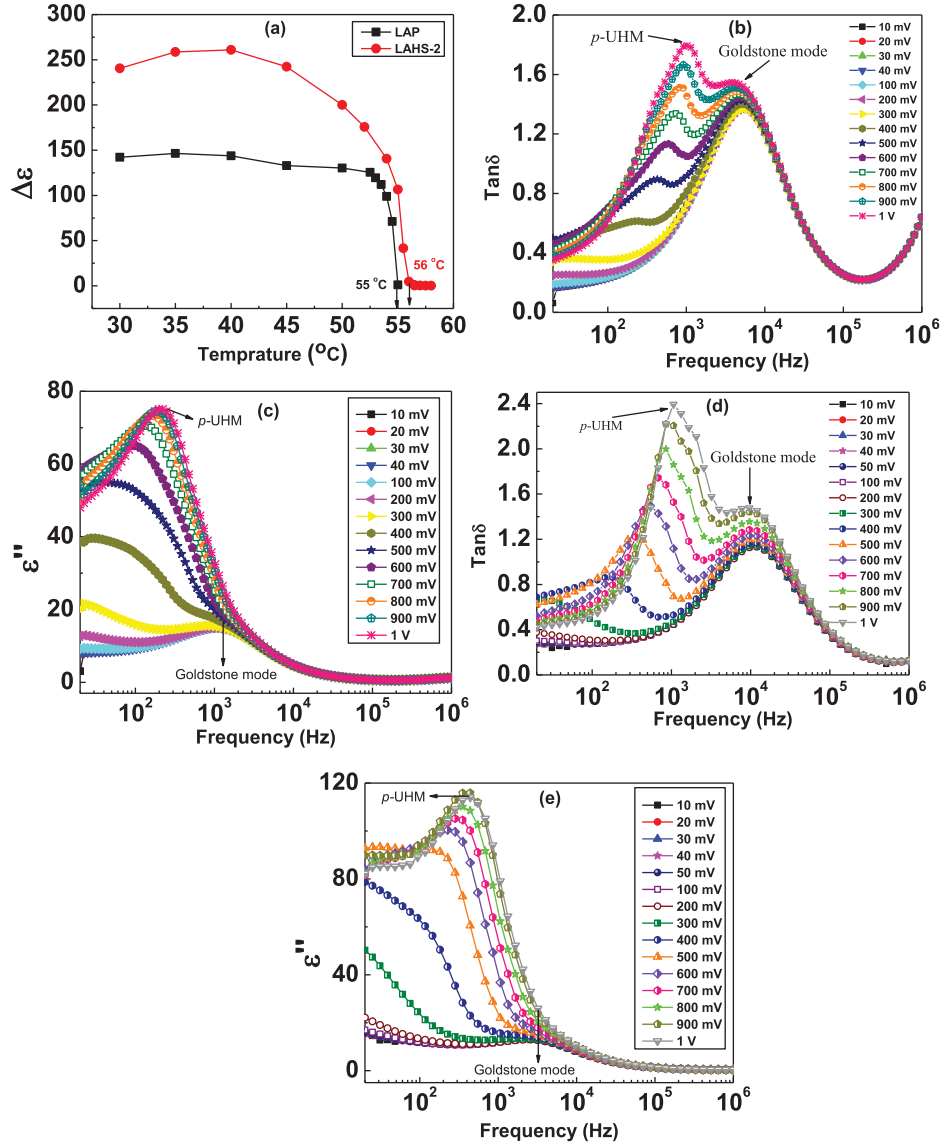

Figure 6. (Colour online) (a) Dielectric strength of DHFLCs at 500 mV, (b) tanδ of LAP-1, (c) imaginary part of complex dielectric permittivity of LAP-1, (d) tanδ of LAHS-2 and (e) imaginary part of complex dielectric permittivity of LAHS-2 as a function of frequency at different applied ac probing voltage.

temperature is saturated to maximum and then starts decreasing with the temperature up to the transition temperature in SmC* phase which is expected because of the diminishing of helix and phase fluctuations near T_c. It is worth pointing out here that the soft mode process also appears in SmC* phase, close to T_c temperature but its magnitude is very small as compared with GM process and is not expected to appear in the current measurement. The GM and *p*-UHM processes at room temperature are shown in both DHFLC materials in Figure 6(b,d) which are taken at different ac voltages at room temperature. As seen in Figure 6(b–e), when both the modes are clearly separated, the dielectric permittivity in SmC* phase is dominated by *p*-UHM process and hence its value reaches to high value.

Relaxation frequency of GM, obtained from data of tanδ versus frequency is plotted as a function temperature in all the materials at 100 and 500 mV probing ac voltage as shown in Figure 7 in SmC* phase. The relaxation frequency of GM is almost independent of temperature in FLCs and LAP-1 at 100 mV ac voltage, whereas in LAHS-2, it decreases with temperature and remains constant near T_c temperature, suggesting that there is another dielectric process (*p*-UHM) in high *Ps* value material [Figure 7(a)]. However, at 500 mV probing voltage, the relaxation frequency of GM process is uniform with temperature in all the FLC materials [Figure. 7(a,b)] suggesting that the *p*-UHM dielectric process is isolated in the extraction of GM in SmC* phase. A significant observation from all four

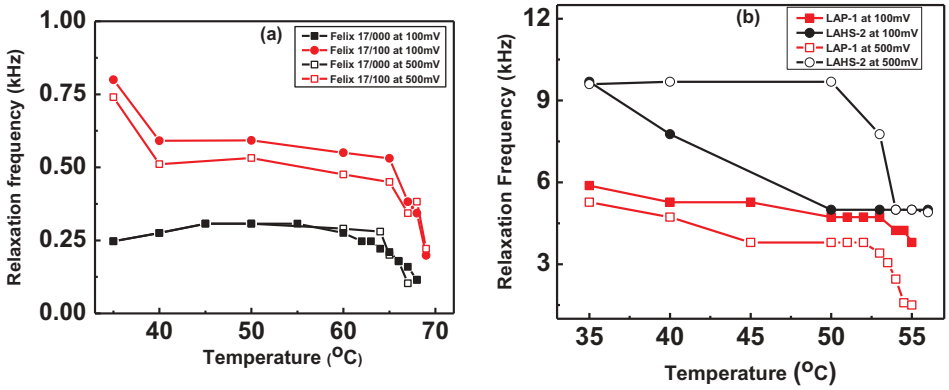

Figure 7. (Colour online) Relaxation frequency of Goldstone mode (a) FLCs and (b) DHFLCs at 100 mV and 500 mV.

materials is that the relaxation frequency is found decreasing near T_c.

Figure 8 shows relaxation process of Goldstone and *p*-UHM processes in Felix 17/100, LAP-1 and LAHS-2 which are obtained from raw data (tanδ versus frequency) and plotted as a function of temperature at 500 mV probing ac voltage in all the materials. However, for low *Ps* value FLC (Felix-17/000), the two processes (GM and *p*-UHM) could not be clearly separated; therefore, it has not been plotted in Figure 8. The *p*-UHM process in another FLC (Felix-17/100) was detected at higher temperatures near T_c only as shown in Figure 8(a). In DHFLCs (LAP-1 and LAHS-2), the relaxation frequency of *p*-UHM process increases with temperature and merges with GM at higher temperature in SmC* phase [Figure 8(b,c)]. As can be seen in Figure 8, the behaviours of GM and *p*-UHM in deep SmC* phase, where the two processes are clearly separated, the two processes, are weakly dependent on temperature. On

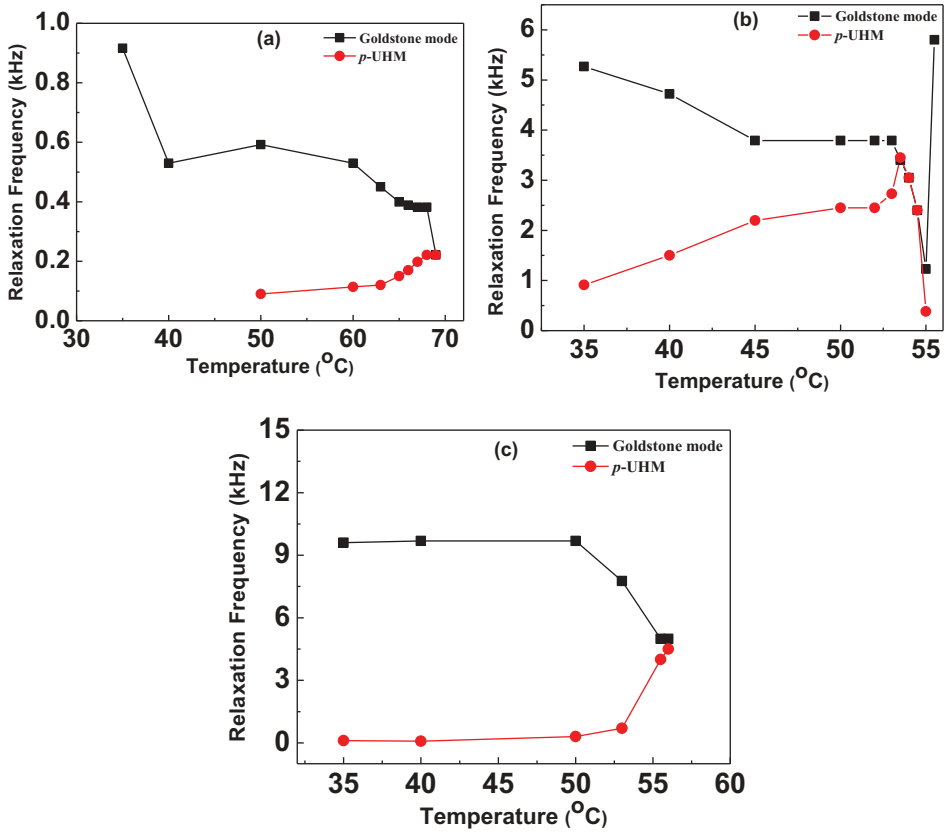

Figure 8. (Colour online) Relaxation frequency of Goldstone mode and *p*-UHM processes at 500 mV of (a) Felix-17/100, (b) LAP-1 and (c) LAHS-2.

the other hand close to T_c, the two processes are observed strongly dependent on temperature. The GM decreases and *p*-UHM increases rapidly near T_c and finally merges together giving a single resultant relaxation process in which the two processes could not be clearly separated. The merging behaviour of GM and *p*-UHM process reveals the coupling nature of two processes under the constraints of strong anchoring, appropriate sample thickness, polarisation value and rotational viscosity.

Conclusion

GM behaviour with temperature is hindered due to the presence of *p*-UHM in SmC* phase in FLC materials. The only behaviour of phason fluctuation (GM) with temperature can be observed when *p*-UHM process is isolated from the overall dielectric permittivity in SmC* phase in higher *Ps* value FLC materials. The *p*-UHM process depends on the *Ps* value of the material in the medium thickness range of highly anchored cells (~8 μm). In low *Ps* FLC materials, GM is dominant whereas in high *Ps* materials, *p*-UHM process dominates. However, in low *Ps* value FLC materials, *p*-UHM process can be detected at high probing field at higher temperature in SmC* phase.

Acknowledgments

We sincerely thank the Director, National Physical Laboratory, New Delhi, for his continuous encouragement in this work. We would like to thank the Department of Science and Technology, New Delhi, India, for financial support through Project Grant GAP-150632 at NPL, New Delhi, India. We sincerely thank Dr A. V. Lapanik of Technical University Darmstadt, Germany, for synthesising deformed helix FLC (LAP-1) material. We sincerely thank Dr A. K. Thakur of Central University of Jammu, India, for useful discussion. A.M.B. and A.B. are thankful to Council of Scientific and Industrial Research (CSIR, India) for the financial assistance under an Emeritus Scheme.

Disclosure statement

No potential conflict of interest was reported by the authors.

Funding

We would like to thank the Department of Science and Technology, New Delhi, India, for financial support through Project Grant GAP-150632 at NPL, New Delhi, India. A.M.B. and A.B. are thankful to Council of Scientific and Industrial Research (CSIR, India) for the financial assistance under an Emeritus Scheme.

References

[1] Beresnev LA, Blinov LM, Osipov MA, et al. Ferroelectric liquid crystals. Philadelphia, PA: Gordon and Breach Science; 1988.
[2] Prakash J, Chandran A, Biradar AM. Scientific developments of liquid crystal-based optical memory: a review. Rep. Prog Phys. 2017;80:016601.
[3] Swaminathan V, Panov VP, Panarin YP, et al. The effect of chiral doping in achiral smectic liquid crystals on the de Vries characteristics: smectic layer thickness, electro-optics and birefringence. Liquid Crystals. 2018;45 (4):513–521.
[4] Fitas J, Dlubacz A, Fryn P, et al. New ferroelectric and antiferroelectric liquid crystals studied by complementary methods. Liquid Crystals. 2017;44(3):566–576.
[5] Levistik A, Carlson T, Filibic C, et al. Goldstone mode and soft mode at the smectic-A – smectic-C' phase transition studied by dielectric relaxation. Phys. Rev. A. 1987;35:3527.
[6] Carlson T, Zeks B, Filipic C, et al. Theoretical model of the frequency and temperature dependence of the complex dielectric constant of ferroelectric liquid crystals near the smectic-C* – smectic-A phase transition. Phys. Rev. A. 1990;42:877.
[7] Hiller S, Beresnev LA, Pikin SA, et al. Dielectric and pyroelectric investigations on the domain mode process in high Ps-FLC Materials. Ferroelectrics. 1996;180:153–163.
[8] Panarin YP, Xu H, MacLughadha ST, et al. Dielectric response of ferroelectric liquid crystal cells. Jpn. J. Appl. Phys. 1994;33:2648–2650.
[9] Khened SM, Prasad SK, Shivkumar B, et al. Dielectric studies of Goldstone mode and soft mode in the vicinity of the A–C transition. J. Phys II. 1991;1:171–180.
[10] Novotna V, Glogarova M, Bubnov AM, et al. Thickness dependent low frequency relaxations in ferroelectric liquid crystals with different temperature dependence of the helix pitch. Liquid Crystals. 1997;23:511–518.
[11] Clark NA, Lagerwall ST. Submicrosecond bistable electro-optic switching in liquid crystals. *Appl. Phys. Lett.* 1980;36:899.
[12] Panarin YP, Kalmykov YP, Lughadha STM, et al. Dielectric response of surface stabilized ferroelectric liquid crystal cells. Phys. Rev. E. 1994;50:4763–4772.
[13] Xu H, Vij JK, Rappaport A, et al. Dynamics of collective and molecular modes of a ferroelectric liquid crystal in confined geometry using dielectric spectroscopy. *Phy. Rev. Lett.* 1997;79:249–252.
[14] Schacht J, Gieselmann F, Zugenmaier P, et al. Dielectric properties of a surface stabilized ferroelectric liquid crystal in cells of various thickness. Ferroelectrics. 1995;173:157.
[15] Choudhary A, Bawa A, Rajesh SP, et al. Dielectric relaxation process of a partially unwound helical structure in ferroelectric liquid crystals. Phys. Rev E. 2017;95:062702.
[16] Kurp K, Czerwinski M, Tykarska M, et al. Design of advanced multicomponent ferroelectric liquid crystalline mixtures with submicrometre helical pitch. Liquid Crystals. 2017;44(4):748–756.
[17] Podgornov FV, Suvorova AM, Lapanik AV, et al. Electrooptic and dielectric properties of ferroelectric

liquid crystal/single walled carbon nanotubes dispersions confined in thin cells. *Chem. Phys. Letts.* 2009;479:206–210.

[18] Takezoe H, Kondo K, Miyasato K, et al. On the methods of determining material constants in ferroelectric smectic C* liquid crystals. Ferroelectrics. 1984;58:1:55–70.

[19] Pikin SA, Yoshino K. Influence of boundaries on the phase transition point in ferroelectric smectics. Jpn. J. Appl. Phys. 1981;20:L-557–L-559.